Assessment of the mechanical performances of Titanium alloys cranial prostheses manufactured by Super Plastic Forming and Single Point Incremental Forming

G. Ambrogio[1], G. Palumbo[2], E. Sgambitterra[1], P. Guglielmi[2], A. Piccininni[2], L. De Napoli[1], T. Villa[3], G. Fragomeni[4]

[1]Dipartimento di Ingegneria Meccanica, Energetica e Gestionale, Università della Calabria

[2] Dipartimento di Meccanica, Matematica e Management, Politecnico di Bari,

[3]Dipartimento di Chimica, Materiali e Ingegneria Chimica "G. Natta", Politecnico di Milano

[4]Università di Catanzaro

Abstract

Custom prostheses are necessary when highly specific and complex geometry regions of the human body have to be replaced. Cranial implants are an example of such patient-oriented prostheses: they are characterised by a medium level of geometrical complexity, quite low thickness, but very important aesthetic and mechanical requirements. In the present work sheet forming processes, i.e. Super Plastic Forming and Single Point Incremental Forming, have been adopted for the manufacturing of custom prostheses, instead of subtractive and additive techniques, which result time and cost consuming when a single-piece batch has to be produced. As concerns the material, three different Titanium alloys were used: pure Titanium and two versions of the alloy Ti-6Al-4V (the Standard one and the Extra Low Interstitial one).

Since no standard protocol exists to assess the mechanical performance of cranial implants, an experimental procedure has been designed and used in this work for producing polymethylmethacrylate supports on which the cranial prostheses were firmly connected and subjected to impact puncture tests (drop tests). An experimental campaign could be thus conducted to investigate the effect on the mechanical response of: (i) the titanium alloy, (ii) the initial blank thickness and (iii) the manufacturing process. Drop tests, carried out according to the proposed procedure, have shown no failure of the prostheses, neither in the area of the impact nor in the anchoring region and have revealed that, irrespective of the adopted manufacturing process, which does not alter the material, the amount of energy absorbed by the implants is always larger than 70%.

Keywords: *SPF; SPIF; pure titanium; Ti-6Al-4V; Ti-6Al-4V-ELI; Drop Test.*

1. Introduction

Recent studies in manufacturing and bioengineering have confirmed the increasing demand for high-quality biomedical implants able to increase the life expectancy of patients and to avoid, at the same time, prolonged hospitalization [1]. Moreover, it is well known that custom implants, which are prostheses able to perfectly fit the damaged region of a specific patient, provide a mechanical connection good enough to avoid relative micro-motions with the surrounding bone region and to prevent the occurrence of infection sites [2]. In addition, custom implants are the gold standard solution when aesthetic compatibility is required, since they ensure very good aesthetic results [3,4]. Cranioplasty, for example, whose aim is to reconstruct structural or morphological cranial regions due to congenital or accidental causes, is a kind of neuro-reconstructive surgery and currently still a challenge for both surgeons and bioengineers. Actually it is a clinical procedure not only for an anatomical reconstruction, but also for the neurological improvement of underlying physiology [5]. Matching the best material and the suitable manufacturing process to obtain a custom implant with higher biomechanical properties is not a trivial question.

Literature offers plenty of data regarding the adoption of several biomaterials, ranging from metals to bioceramics [6] and biopolymers [7], but titanium (Ti) and its alloys still remain the most widely adopted solution since they possess a low value of the Young's modulus (thus assuring an homogeneous stress distribution between the implant and the surrounding bone [8,9]), excellent mechanical properties and moreover, as far as biocompatibility is concerned, the capability of promoting osseointegration [10,11].

Concerning the production process, stereolithography [12] and the CAD/CAM approach [13,14] are considered highly effective for manufacturing bioimplants since such processes facilitate, speed up and improve the quality of surgical procedures. On the other hand, especially when the geometry of the prosthesis is characterised by thin walls and extreme complexity (even undercuts), sheet metal forming processes, such as the Super Plastic Forming (SPF) and the Single Point Incremental Forming (SPIF) can be, as confirmed by the literature, valid alternatives to the conventional subtractive ones [15].

It has to be pointed out that the overall quality of a prosthetic implant is based not only on its fitting and connection characteristics, but also on its structural properties. For this

reason, it is fundamental to assess the load-bearing capacity of the implant. The structural requirements of medical devices can widely vary when changing the loads the device is subjected to after the implantation. In some cases the magnitude of such loads can be very high (e.g. in a hip prosthesis it can reach five times the value of the body weight while in dental implants can reach almost 1kN) being then resolved in a stress state dependent on both the final dimension and the geometry of the implant. The high stresses that can arise in an implantable device, regardless of the material it is made of, can in turn promote different failure mechanisms which lead to replace the device. Among the different failure mechanisms related to mechanical issues, wear, static and fatigue failures are the most common. Examples can be found in the replacements of knee where wear is the major cause of revision, due to very high contact stresses in the polyethylene insert [16]. As far as static failures are concerned, due to the high magnitude of contact pressures in the hip joint, some examples of collapses of the ceramic components of hip prostheses can be found [17], while fatigue failure still mostly affects the metallic stem [18] or neck of such a kind of prosthesis [19]. Other examples of failures due to demanding mechanical stimuli can be cited for different materials: fatigue failures of Nitinol peripheral stents still affect their survivorship [20] and expose the patient to the need for a new surgery. Most medical implants require very specific properties. An arterial graft, for instance, needs to offer flexibility, anisotropic behaviour and compliance which match that one of the adjacent vessel [21]. A balloon angioplasty catheter needs to be tractable over a guide wire and must be stiff enough to prevent kinking and flexible enough to navigate the vasculature. Sutures need to provide high tensile strength and in case of resorbable sutures, this strength must decrease over time in a controlled manner. Orthodontic wires require high elastic limit and low stiffness, because they provide the ability of applying lighter and more constant forces during arch deactivation [22].

Cranial prostheses, instead, require low stiffness and high toughness in order to guarantee a good distribution of the stresses and to better absorb accidental impact [23]. For such reasons, the structural properties of the biomaterials and the way they are manufactured are extremely important for the long-term success of the implant. In addition, ad-hoc experimental setup and equipment are required to characterize the specific application of biomedical implants. For some of them, approved standards are available: for example, for evaluating the static and fatigue behaviour of lower limb orthopaedic prostheses [24] and devices for spinal surgery [25], or for determining the wear behaviour of components used in total joint prostheses [26], or for the measuring the corrosion fatigue of metallic

implants [27].

On the other hand, when dealing with cranial implants, there is a lack of standards able to provide testing procedures for their mechanical characterization; such a lack is probably due to the fact that such cranial implants do not bear loads during their use, but they can be only accidentally overloaded because of fortuitous falls or during sports activities. In this context, only few studies report procedures to assess the structural performance of cranial prostheses For example, Tsouknidas et al. investigated the mechanical response of implants subjected to an additional load simulating the impact of a tennis ball at a reference speed of 30 m/s [28]; Garcia-Gonzalez et al. [29] simulated the impact conditions of an accidental fall (for instance from the bed or the bike) on polyether-ether-ketone and macro-porous hydroxyapatite implants.

In this work the mechanical performance of Ti cranial prostheses manufactured by SPF and SPIF has been assessed by means of impact puncture tests carried out using an universal INSTRON drop test machine. For this aim, a proper setup has been designed to perform the impact experiments and three different Ti alloys have been investigated: pure Titanium and two versions of the alloy Ti-6Al-4V (the standard one and the Extra Low Interstitial one). Since no standard actually exists for assessing the mechanical performance of cranial implants, a new experimental procedure has been designed and used in this work for producing polymethylmethacrylate (PMMA) supports on which the cranial prostheses were firmly connected and subjected to drop tests. An experimental campaign was thus conducted adopting two different load conditions in order to investigate the effect on the mechanical response of: (i) the titanium alloy, (ii) the blank initial thickness and (iii) the manufacturing process.

2. Material, experimental setup and procedure

2.1. The investigated case study

The following *Figure 1* shows the steps required for the definition of the geometry of the prosthesis adopted in the present work as case study.

Starting from a polymer model anatomically identical to the human skull, a defect in the apex frontal area was created (*Figure 1*a). By means of the damage acquisition (*Figure1*b) and the subsequent reconstruction using mirroring techniques (*Figure 1*c), the prosthesis geometry, able to fill the bone defect, was defined and subsequently extended for ensuring the optimal anchoring system [30].

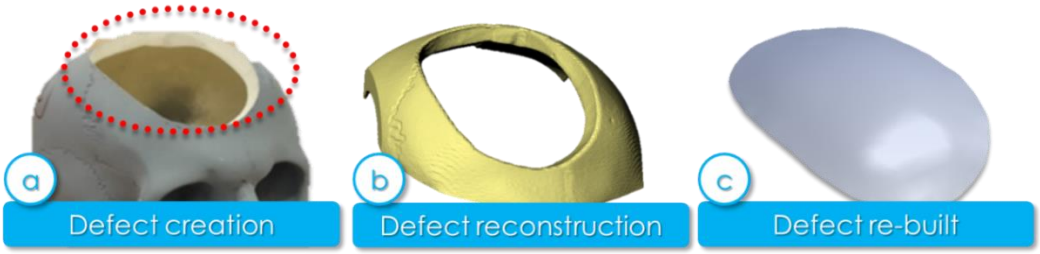

Figure 1. Case study.

Three Ti alloys, largely adopted for biomedical devices, were investigated in the present work: the commercial pure Ti (Ti-Gr2), the Ti-6Al-4V (Ti-Gr5), and the Extra Low Interstitial Ti-6Al-4V (Ti-Gr23). The chemical compositions of the investigated alloys are presented in Table 1.

Table 1. Chemical composition of the investigated Ti alloys

Alloy	Al [%]	V [%]	Fe [%]	C [%]	N [%]	H [%]	O [%]	Ti [%]
Ti-Gr2	-	-	0.3 max	0.10 max	0.03 max	0.015 max	0.3 max	Bal.
Ti-Gr5	5.5 - 6.5	3.5 - 4.5	0.3 max	0.08 max	0.05 max	0.015 max	0.2 max	Bal.
Ti-Gr23	5.5 - 6.5	3.5 - 4.5	0.25 max	0.08 max	0.05 max	0.015 max	0.13 max	Bal.

Both the SPIF and SPF processes were adopted to manufacture prostheses made of Ti-Gr5 (1 and 1.5mm thick); on the contrary, prostheses made of Ti-Gr2 (1.5mm) and Ti-Gr23 (1mm) were manufactured only by SPIF and SPF, respectively. This choice is justified by the opportunity of investigating both processes when the material properties change. According to that, Ti-Gr2 was adopted for testing also the SPIF feasibility in cold condition, whereas Ti-Gr23 was chosen for its superplastic behaviour, suitable for SPF operations.

A prior investigation of all the adopted materials was made by using flat samples. In particular, preliminary tests were performed on Ti-Gr2 and Ti-Gr5 using flat samples 1.0 and 1.5 mm thick, and on Ti-Gr23, using flat samples 1.0 mm thick.

2.2. Hardness tests

In order to determine the mechanical properties of the investigated Ti alloy sheets in the as received conditions, Vickers microhardness tests were carried out.

Tests were performed according to the UNI EN ISO 6507-1 Standard [31]. The HWMMT-X7

micro hardness tester by HIGHWOOD was used and a load of 1,000 g was chosen. Six replications were performed on each sample.

2.3. Experimental setup for prostheses manufacturing

SPF experiments were conducted using the 2,500 kN prototypal electro-hydraulic press machine shown in Figure 2a. Forming tools were heated by means of electric cartridges managed by a PLC. As shown in Figure 2b, in the upper tool a metallic insert, with a cavity having the geometry of the case study, was used. Before each test, boron nitride was applied on both blank surfaces in order to simplify the extraction of the formed part.

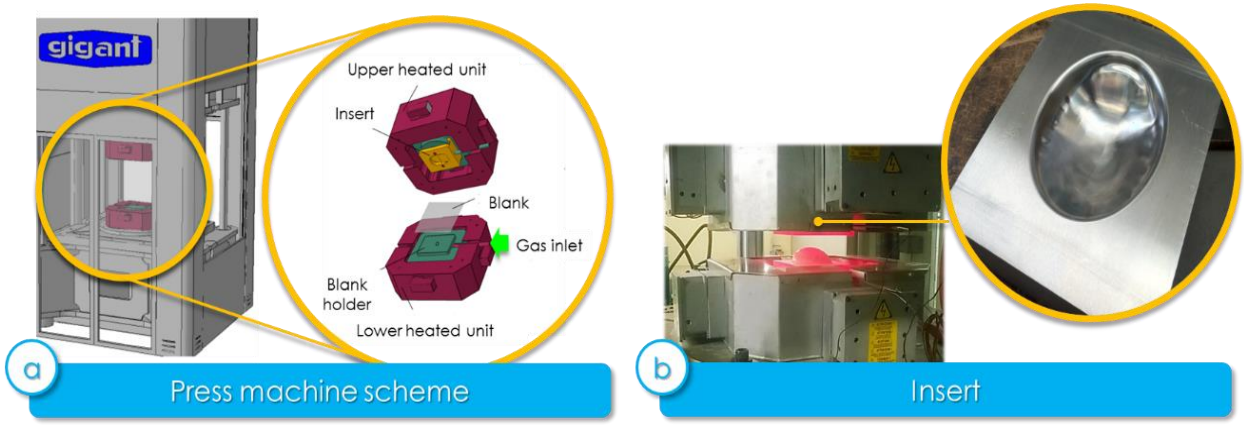

Figure 2. Experimental set-up for SPF.

Temperatures were monitored during the process using K-type thermocouples positioned in both the upper and the lower tool. When the forming temperature (850 °C) was reached [32], the blank was introduced between the tools and then clamped (a blankholder force of 490 kN was used for preventing any drawing and gas leakage). The blank was formed by the gas whose pressure was set according to an optimized pressure profile obtained from numerical simulations using ABAQUS and properly modelling the material superplastic behaviour [15,33]. In particular, for each of the adopted alloys (Ti-Gr23 1.0 mm thick, Ti-Gr5 1.0 mm thick and Ti-Gr5 1.5 mm thick) the pressure profiles shown in Figure 3, able to keep the strain rate close to the optimal value, were determined using an ABAQUS built-in subroutine and implemented in the press machine as a list of values (time-pressure).

SPIF experiments were performed on a 3-axis CNC MAZAK milling machine. The adopted equipment is sketched in *Figure 4*. As shown in *Figure 4*a, the standard SPIF clamping frame was equipped with an additional electrical heater which allowed to conduct the process in hot-condition. The high temperature, in fact, is mandatory for obtaining sound results when processing the Ti-Gr5.

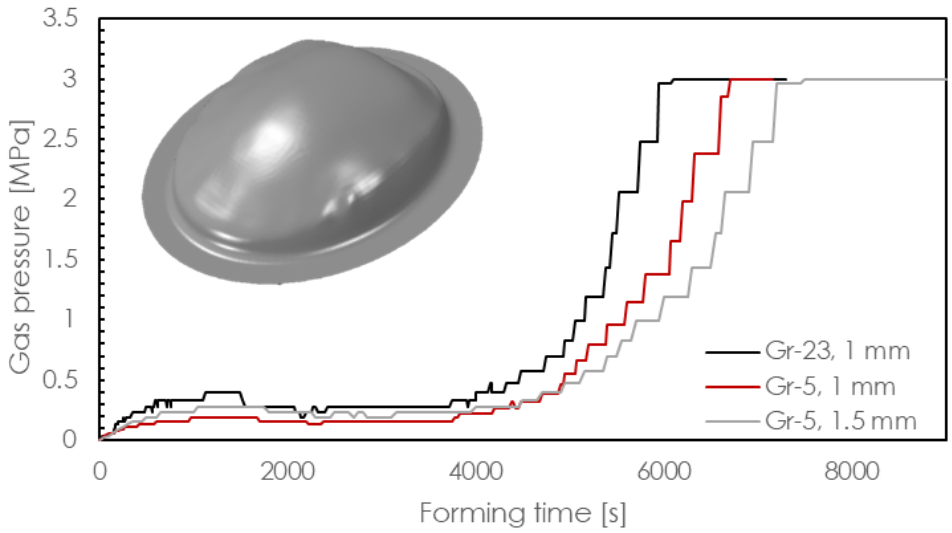

Figure 3. Optimized pressure profile obtained from numerical simulation for the SPFed prostheses.

The original clamping frame was thus enriched with a 2kW electric heater and insulated in order to reduce heat losses to the environment and to the working table (*Figure 4*b). In this way, by using the same equipment, the process was performed both at room temperature (without any heating source) for manufacturing the Ti-Gr2, and in hot conditions for processing the Ti-Gr5.

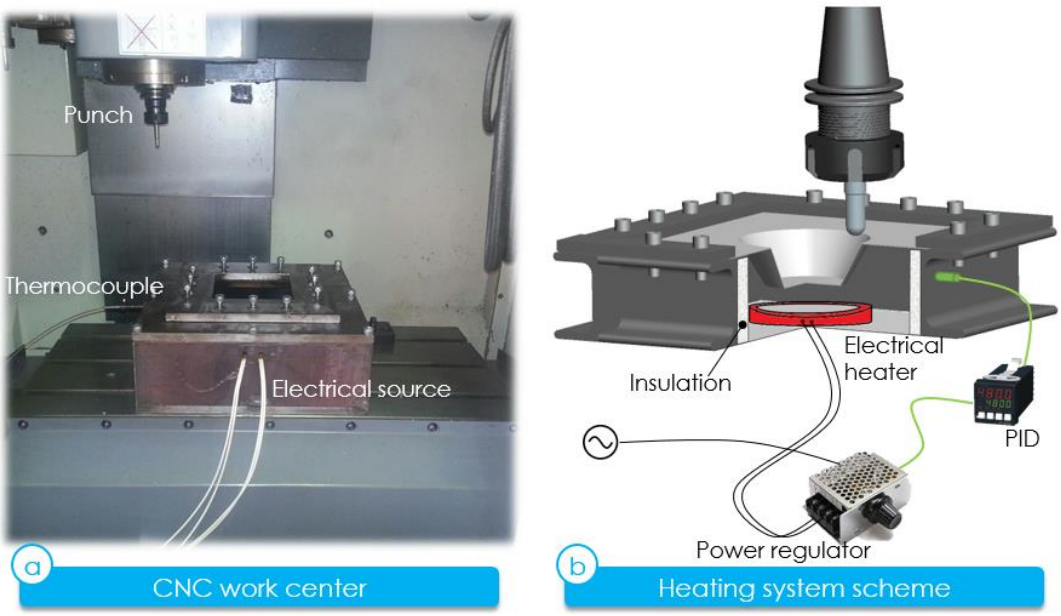

Figure 4. Experimental set-up for SPIF.

To perform the hot SPIF in the proper way, a pair of thermocouples positioned in the chamber and on the sheet was utilised to control the temperature. At the initial stage of the experiments, a FLIR thermo-camera was used to check and properly calibrate the PID

controller of the electrical heater: a temperature of 650°C was reached during the forming phase and properly kept constant during the manufacturing. A hemispherical HSS tool with a diameter of 12 mm was adopted. The sheet was deformed according to a tool trajectory previously defined by means of numerical simulations. Regardless of the adopted temperature, all tests were performed using a constant tool pitch equal to 0.5 mm, a tool feed rate of 2.5 m/min and a tool rotational speed of 600 RPM.

After the manufacturing step, both SPFed and SPIFed parts were cut by means of a 3D laser in order to extract the final geometry from the formed blank; using the same fixture, the laser drilling of eight holes for the anchoring to the PMMA support was also performed. The laser cutting path and the position of the holes (approximately at an angular distance of 45° each other) are shown in Figure 5.

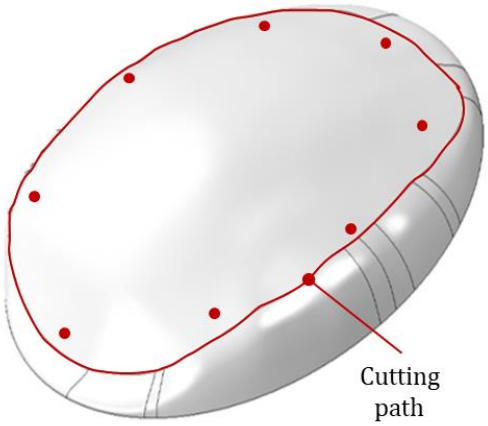

Figure 5. Cutting path and position of the holes.

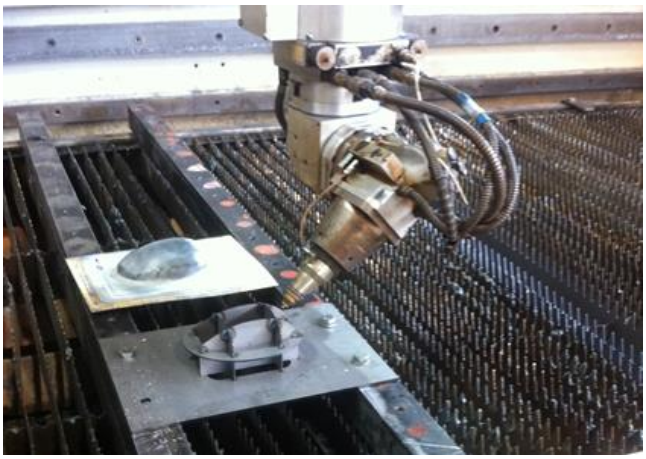

Figure 6. Formed blank positioning for the 3D laser cutting of SPFed and SPIFed parts.

After preliminary cuts on flat specimens to tune the laser parameters, the following ones (able to minimize burrs) were adopted: laser power=400 W, nitrogen pressure=12 bar, cutting speed=1 m/min, focal length=4 mm, stand-off distance=1.2 mm. In Figure 6 the set up adopted for the laser cutting operation is shown.

2.4. Drop tests

2.4.1. Preparation of the support and anchoring of the prosthesis

Drop tests were performed on SPFed and SPIFed prostheses connected on purposely made anchoring supports whose geometry was made identical to the upper portion of the defected skull. Both the way to produce such supports and the material they were made of, were chosen according to the need of having a large number of them and, at the same time,

of producing them in a robust and repeatable way. The procedure illustrated in Figure 7 shows the supports manufacturing using a synthetic resin (PMMA, also known as "bone cement") which was poured into a SPFed formed blank used as mould.

Figure 7. Procedure of support manufacturing.

The choice of PMMA as material for the supports was due to the fact that this biomaterial is commonly used to connect the prosthesis to the host bone since it has mechanical characteristics very similar to the human bone.

In order to create in the support the hole accounting for the defect, a proper shaped core, having approximately the dimension of the defect, was positioned in the cavity before pouring the PMMA. After the resin curing, the support was extracted and four bushes were inserted in the bottom surface so that it could be rigidly coupled with the standard clamping system of the drop test machine by means of four screws. The anchoring of the SPFed and SPIFed prostheses to the supports was made mimicking the surgical technique: as reported in Figure 8, four standard self-cutting 2.0 mm titanium cortical screws were used to connect the prosthesis to the PMMA support.

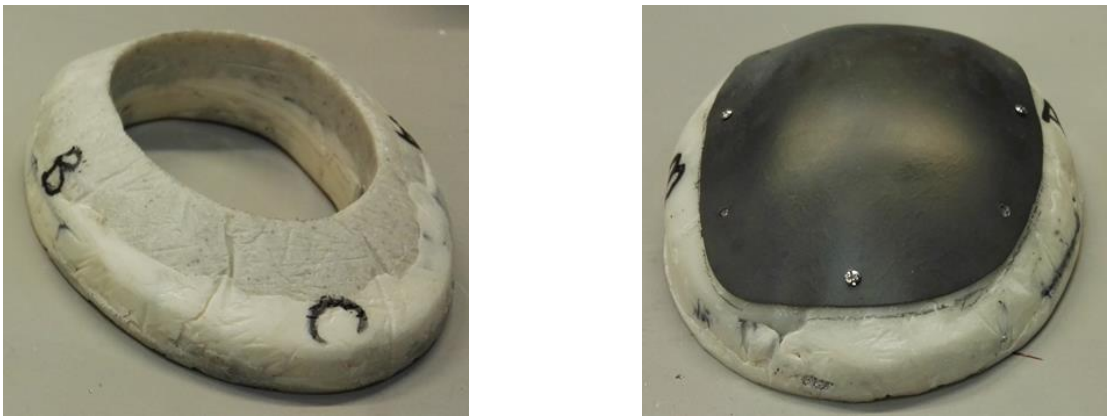

a) b)

Figure 8. Anchoring of the prosthesis: a) PMMA support, b) anchored prosthesis.

2.4.2. Drop tests equipment

Drop tests were performed on the 3D laser cut prostheses using an Instron CEAST 9350 drop tower, which is able to perform impact experiments applying energies up to 1,800 J by means of a spring assist. An instrumented striker equipped with a polished 20 $\pm$ 0.2 mm hemispherical nose impactor (mass: 2.295 kg) was employed in the present work. Due to the non-standard shape of the samples, the purposely made supports described in the section 2.4.1 were used to firmly connect the prostheses and thus to minimize vibrations during the test. In particular, the support on which the prosthesis was anchored, was connected to the clamping system shown in Figure 9, made of a plate having four columns able to carry an additional upper plate used to avoid vibrations during the impact.

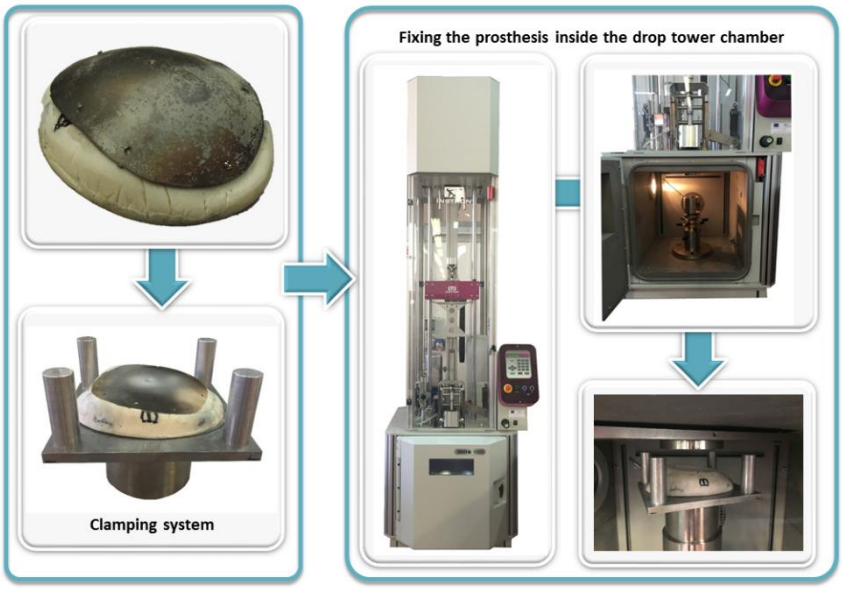

Figure 9. Set up for drop tests.

All components were properly designed in order to guarantee high stiffness of the whole system. After the first impact of the specimen, a break mechanism automatically prevented a second strike. During the impact, the resistive force exerted by the specimen was measured by a 45 kN strain gauge load cell.

Experiments were conducted adopting two different falling heights (h) for each specimen type: 200 and 600 mm, corresponding to nominal impact energies (E_{max}) and velocities (v_i) of 4.5 J - 1.98 m/s and 13.5 J -3.43 m/s, respectively. Such values can simulate a possible daily accident. At least three tests were performed for each load condition.

From the basic force–time information, important parameters such as deflection, $\delta(t)$, absorbed energy, $E(t)$, and velocity, $v(t)$ were calculated. The velocity versus time was evaluated by using Eq. (1) [34]. A positive velocity value indicates a downward motion.

$$v(t) = v_i + gt - \int_0^t \frac{1}{m} F(t)dt \qquad (1)$$

where t is the time; $v(t)$ and v_i are the impactor velocities at time t and t=0, respectively; $F(t)$ is the measured impactor contact force at time t; m is the mass of impactor. The deflection $\delta(t)$ versus time was calculated through Eq. (2) [34].

$$\delta(t) = \delta_i + v_i t + \frac{gt^2}{2} - \int_0^t \int_0^t \frac{1}{m} F(t)dt \qquad (2)$$

where $\delta(t)$ and δ_i are the impactor displacements from the reference location at time t and t=0, respectively. The absorbed energy $E(t)$ versus time was calculated through Eq. (3) [34]:

$$E(t) = \frac{m(v_i^2 - v(t)^2)}{2} + mg\delta \qquad (3)$$

where $E(t)$ is the absorbed energy at time t.

2.4.3. Output of the drop tests

Figure 10 shows the typical responses obtained from an instrumented impact test. In particular, Figure 10a shows both the force and the energy response as a function of the time, while Figure 10b shows the acquired force according to the sample deflection.

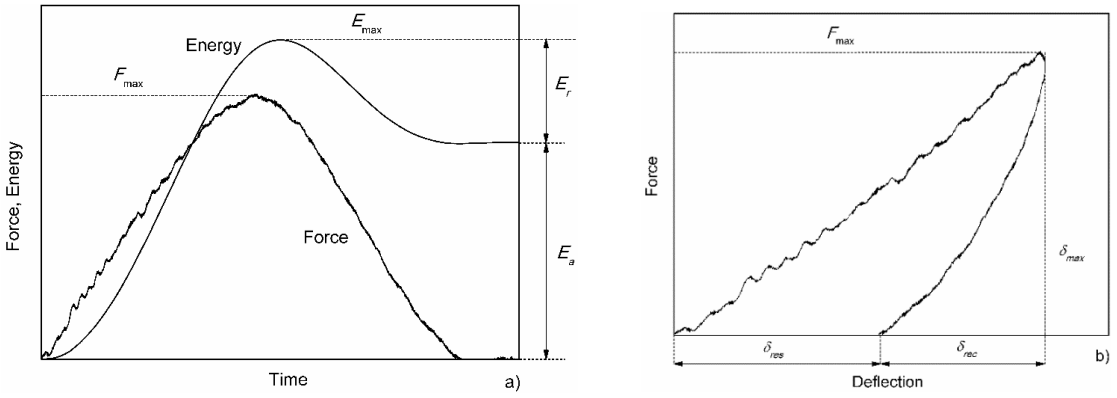

Figure 10. Responses obtained from instrumented impact test: a) force and energy vs time, b) force vs deflection.

In the figures, all the investigated parameters are also shown: F_{max} (the maximum force), E_{max} (the maximum amount of energy that is absorbed by the specimen), E_r (the rebound energy, i.e. the energy returned by the sample to the punch), E_a (the total energy absorbed

by the sample), δ_{max} (the maximum deflection), δ_{res} (the residual deflection) and δ_{rec} (the recovered deflection).

In order to compare the behaviour of different materials, even characterised by a different thickness, the following assitional parameters revealed to be necessary and thus used in the present work: the absorbed energy ratio (i.e. the absorbed energy over the maximum applied energy, E_a/E_{max}) and the residual deflection ratio (i.e. the residual deflection over the maximum recorded one, $\delta_{res}/\delta_{max}$).

3. Results and Discussion

3.1. Assessment of mechanical characteristics of the as received sheets

Results on samples extracted from the sheets of the investigated Ti alloys in the as-received condition are plotted in Figure 11 as mean values.

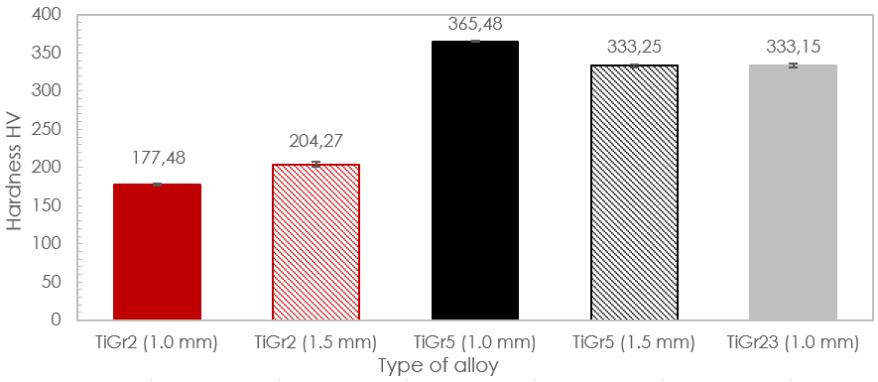

Figure 11. Micro-hardness average values of the investigated Ti alloy in the as received condition.

The hardness levels revealed that the thickness always affects the mechanical behaviour, even in case of the same alloy. For example, the alloy Ti-Gr5 1.0 mm thick has a hardness level about 10% greater than the Ti-Gr5 1.5 mm thick. The opposite can be noted when comparing the hardness of the two samples in Ti-Gr2: the 1mm thick has a hardness level about 10% lower than the 1.5mm. Such differences appear to be a consequence of the production process the sheet was subjected to, thus revealing the necessity of assessing the material behaviour before the investigation on the formed blanks.

3.2. Drop tests on flat samples

Preliminary tests, using the drop tower described in the section 2.4.2, were performed on flat samples in order to evaluate the impact response of the investigated materials in the as received condition. In particular, disk-shaped samples with a diameter of 60 mm were cut

from the sheets and clamped on a support ring with an internal diameter of 40 ± 2 mm. The same testing parameters adopted to analyse the prostheses (see section 2.4) were used. Table 2 resumes the obtained results (average data) in terms of: (i) energy, (ii) deflection and (iii) maximum force acquired during the tests; furthermore, the absorbed energy ratio (E_a/E_{max}) and the residual deflection ratio ($\delta_{res}/\delta_{max}$) are also shown.

Table 2. Resume of results obtained from impact tests on flat samples.

Specimen	Falling height [mm]	E_{max} [J]	E_r [J]	E_a [J]	F_{max} [N]	δ_{max} [mm]	δ_{res} [mm]	δ_{rec} [mm]	E_a/E_{max}	$\delta_{res}/\delta_{max}$
Gr2–1mm	200	4.50	0.50	4.00	3,154.79	2.96	2.49	0.47	0.89	0.84
	600	13.50	0.80	12.70	6,327.48	4.52	4.2	0.32	0.94	0.93
Gr2–1.5mm	200	4.50	0.60	3.90	3,666.86	1.97	1.56	0.41	0.86	0.79
	600	13.50	0.95	12.55	6,946.98	3.43	3.04	0.39	0.93	0.89
Gr5–1mm	200	4.50	1.39	3.11	3,749.22	2.53	1.42	1.11	0.69	0.56
	600	13.50	2.78	10.72	8,117.94	3.82	2.65	1.17	0.79	0.69
Gr5–1.5mm	200	4.50	1.27	3.23	4,092.99	1.91	1.07	0.85	0.72	0.56
	600	13.50	2.07	11.43	7,892.34	3.24	2.20	1.04	0.85	0.68
Gr23–1mm	200	4.50	1.10	3.40	3,720.57	2.66	1.79	0.87	0.75	0.67
	600	13.50	2.25	11.25	7,856.53	4.06	3.10	0.97	0.83	0.76

The graphs in Fig xx show the effect of the thickness on the maximum deflection when using samples made of different alloys (Gr2 and Gr5) and setting different load conditions.

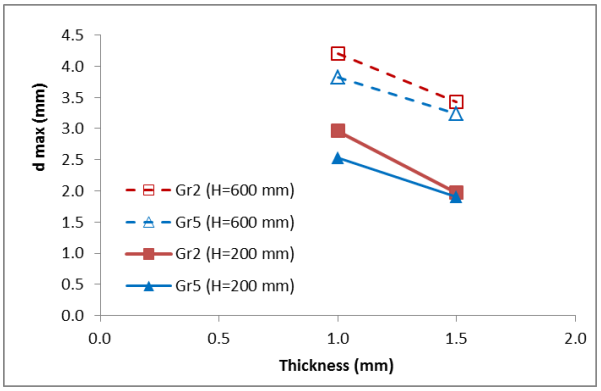

Fig xx

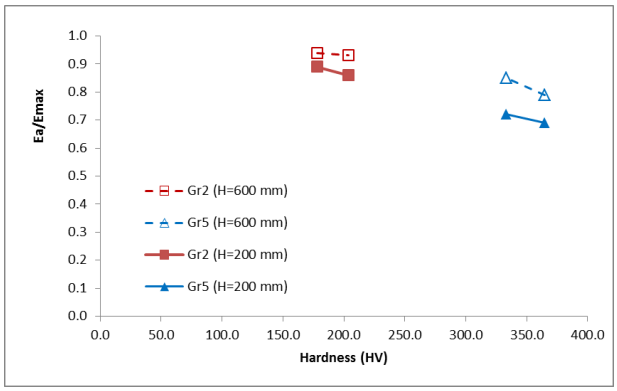

Fig yy

It is possible to note that when increasing the thickness, irrespective to the material strength revealed by hardness measurements (figure 11), the deflection level is reduced (it is simply related to the the Young modulus and to the thickness). In figure yy, on the

contrary, the effect of hardness on the ratio Ea/Emax is shown for both Gr2 and Gr5 and for both the load conditions: it is worthy of notice that such a parameter inversely affects the amount of energy which is stored by the sample.

The graphs in Figure 12 show the comparison among the three investigated Ti alloys (with the same thickness of 1.0 mm) in terms of maximum force (Figure 12a), residual deflection (Figure 12b), absorbed energy ratio (Figure 12c) and residual deflection ratio (Figure 12d). It is possible to note that the investigated parameters are directly affected by the load condition and their values increase according to the falling height. Furthermore, results show that Ti-Gr2 exhibits the highest deformation, as highlighted by the maximum deflection value reported in Figure 12b for both the load conditions, but also the highest capability in absorbing energy and recovery deflection compared to the other alloys (Figure 12c and Figure 12d).

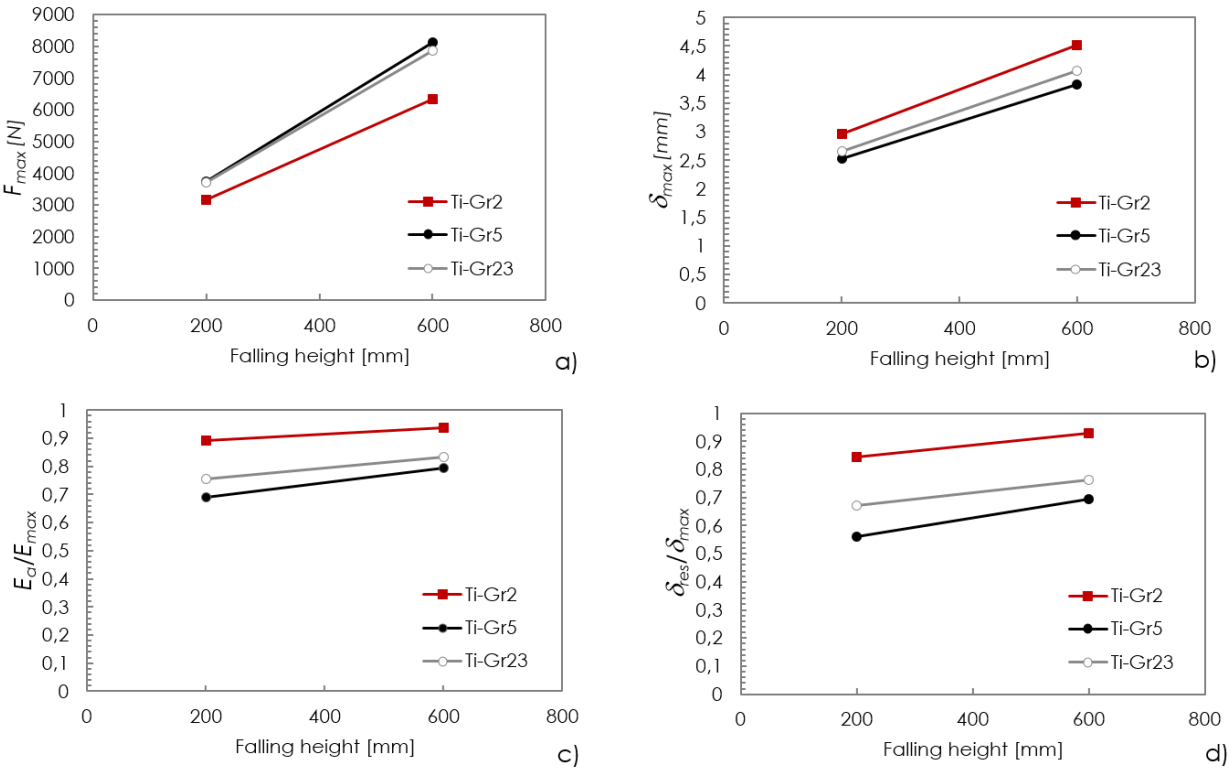

Figure 12. Comparison between the three investigated Ti alloys (thickness of 1.0 mm).

Such results are in good agreement with the mechanical response assessed by micro-hardness tests (Figure 11), which revealed that the Ti-Gr2 possess the lowest hardness.

In Figure 13 the same parameters have been considered, but the attention has been focused only on Ti-Gr2 and Ti-Gr5 and on the thickness variation.

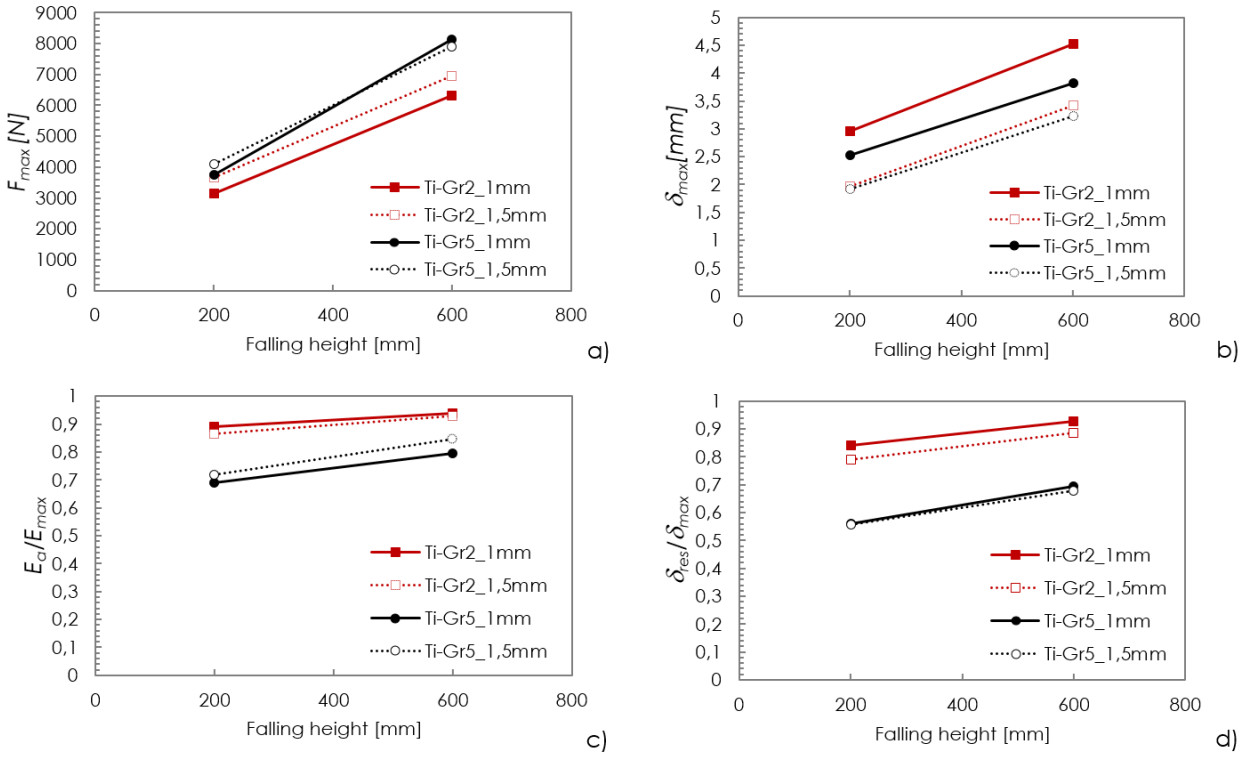

Figure 13. Comparison when changing the Ti alloy and the sheet thickness.

Results show that for both the alloys the maximum force registered increases at the thickness increase as far as the maximum deflection on the sample decreases. However, both effects are much more evident on Ti-Gr2 which is characterised by a more significant strength increase at the higher thickness with respect to the Ti-Gr5. At the same time, the Ti-Gr2, in both thickness configurations, is always able to absorb the highest energy and, as a direct consequence, it shows the largest residual deflection ratios. When dealing with the Ti-Gr5 and different thicknesses, an interesting behaviour can be observed too, as Figure 13 reveals: irrespective of the larger thickness of the Ti-Gr5, the sample 1.5 mm thick was able to absorb a bit more energy than the sample 1.0 mm thick; in addition, negligible differences could be noted for such an alloy in terms of residual displacement ratio between the thick and the thin samples. All these behaviours can be in this case explained by the hardness values and in particular by the higher hardness showed by the Ti-Gr2 1.5 mm with respect to 1.0mm and the absolute highest value of the hardness measured on Ti-Gr5 1.0 mm thick.

3.3. Drop Tests on cranial prostheses

An extensive experimental campaign was conducted on the prostheses manufactured using the investigated sheet forming processes. In particular, each cranial implant was tested

using the setup and the testing conditions detailed in section 2.4. Three replications for each test were performed. According to Table 3, six different configurations were investigated and a total amount of 36 cranial prostheses were tested.

Table 3. Summary of the performed drop test

	Process	SPF		SPIF	
	Height of fall	200mm	600mm	200mm	600mm
Material Type	Ti-Gr2, 1.5mm	-	-	Done	Done
	Ti-Gr5, 1mm	Done	Done	Done	Done
	Ti-Gr5, 1.5mm	Done	Done	Done	Done
	Ti-Gr23, 1mm	Done	Done	-	-

A typical response obtained from the impact test is reported in Figure 14.

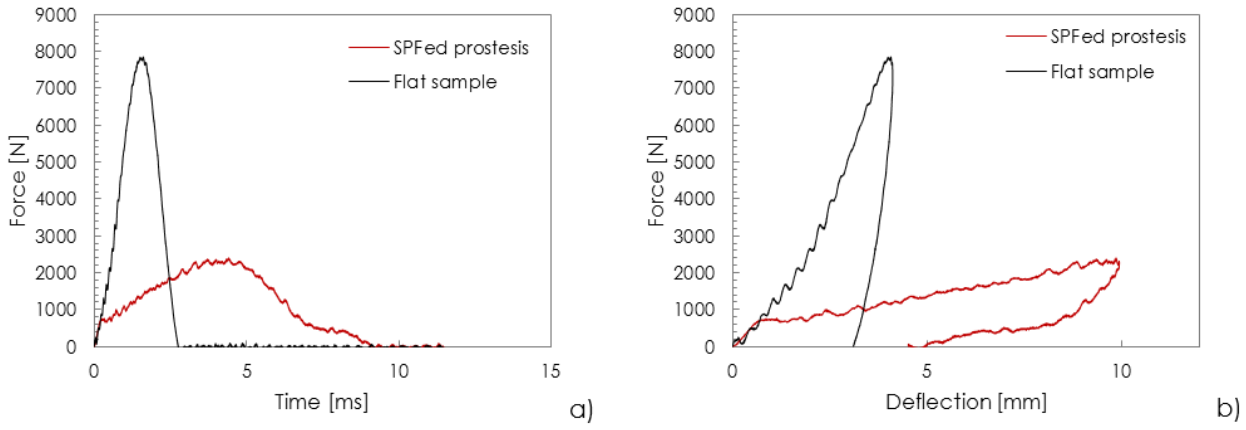

Figure 14. Responses from instrumented impact test performed on Ti-Gr23, 1mm thick: a) force vs time, b) force vs deflection.

In particular, Figure 14a shows the acquired force during the test conducted on the prosthesis made of Ti-Gr23 1.0 mm thick subjected to an impact energy of 13.5 J, while in Figure 14b the force and the deflection acquired in the same test have been combined. Furthermore, in both figures analogous results obtained from the test conducted on a flat sample (same alloy and thickness) have been plotted. Figure 14 highlights that both samples (the flat and the formed one) exhibit a similar response (increasing trend) only up to a certain force level; after that, bending instability occurred on the prosthesis, due to its specific shape, thus determining an evident change in the slope of the curves.

In Table 4 a summary of the main results obtained from the drop tests are presented. Both average and standard errors concerning the deflection are reported for the sake of clarity.

Table 4. Summary of the results obtained from impact tests on cranial prostheses

Specimen	Falling height [mm]	E_{max} [J]	E_a [J]	E_R [J]	F_{max} [N]	δ_{max}		δ_{res}		E_a/E_{max}	$\delta_{res}/\delta_{max}$
						Ave [mm]	StdErr*	Ave [mm]	StdErr*		
SPIF_Gr2–1.5mm	200	4.50	3.90	0.60	3058.10	1.90	0.00	1.50	0.00	0.87	0.79
	600	13.50	12.35	1.15	4218.32	4.42	0.04	3.87	0.09	0.91	0.88
SPIF_Gr5–1mm	200	4.50	3.34	1.16	2159.29	3.54	0.00	2.30	0.00	0.75	0.65
	600	13.50	10.50	3.00	3303.40	6.47	0.01	4.08	0.12	0.78	0.63
SPIF_Gr5–1.5mm	200	4.50	3.50	1.00	3552.27	1.98	0.00	1.33	0.00	0.78	0.67
	600	13.50	11.32	2.18	4712.49	4.13	0.53	3.13	0.28	0.84	0.76
SPF_Gr5–1mm	200	4.50	2.65	1.85	1400.14	4.97	0.00	2.17	0.00	0.59	0.44
	600	13.50	9.30	4.20	2461.88	9.09	0.39	3.98	0.05	0.69	0.44
SPF_Gr5–1.5mm	200	4.50	3.31	1.19	2503.06	2.85	0.00	1.67	0.00	0.74	0.57
	600	13.50	10.50	3.00	3484.23	6.13	0.11	3.84	0.28	0.78	0.63
SPF_Gr23–1mm	200	4.50	2.90	1.60	1514.73	4.35	0.00	2.00	0.00	0.65	0.46
	600	13.50	10.45	3.05	2399.22	9.69	0.16	4.93	0.03	0.76	0.51

* StdErr is the standard error measured as the ratio: $\frac{Stand\ Dev}{\sqrt[2]{n}}$, where *n* is the number of replications.

It is worthy of notice that all the investigated implants safely absorbed the applied energy without any crack insurgence: no fracture occurred neither in the region of the impact nor in the anchoring region where titanium cortical screws, connecting the prosthesis to the PMMA support, were positioned. In Figure 15, two samples tested with the highest impact conditions (i.e. falling height of 600mm and impact energy of 13.5 J) are reported for SPFed and SPIFed parts made with Ti-Gr5 1mm thick.

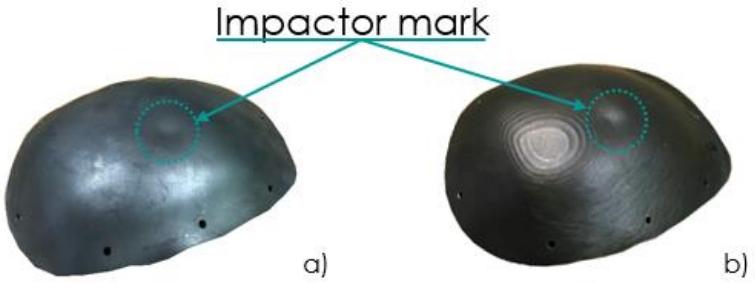

Figure 15. Samples produced by a) SPF and b) SPIF as result after the impact test.

3.3.1. Effect of the Ti alloy

The graphs in Figure 16 show a direct comparison of the results in terms of maximum

deflection value and ratios E_a/E_{max}, and $\delta_{res}/\delta_{max}$ concerning the SPFed prostheses in Ti-Gr5 and Ti-Gr23 (both with an initial thickness of 1.0mm) when subjected to the two load conditions.

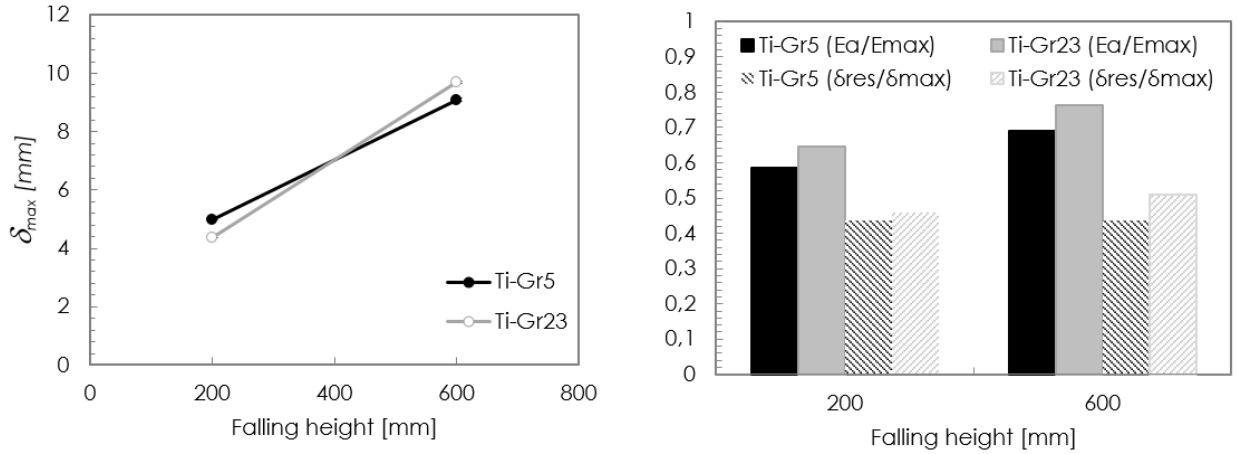

Figure 16. Comparison between SPFed prostheses in Ti-Gr23 and Ti-Gr5 (1.0 mm thick).

Figure 17 shows the same comparison but concerning the SPIFed prostheses in Ti-Gr5 and Ti-Gr2 (both with an initial thickness of 1.5mm).

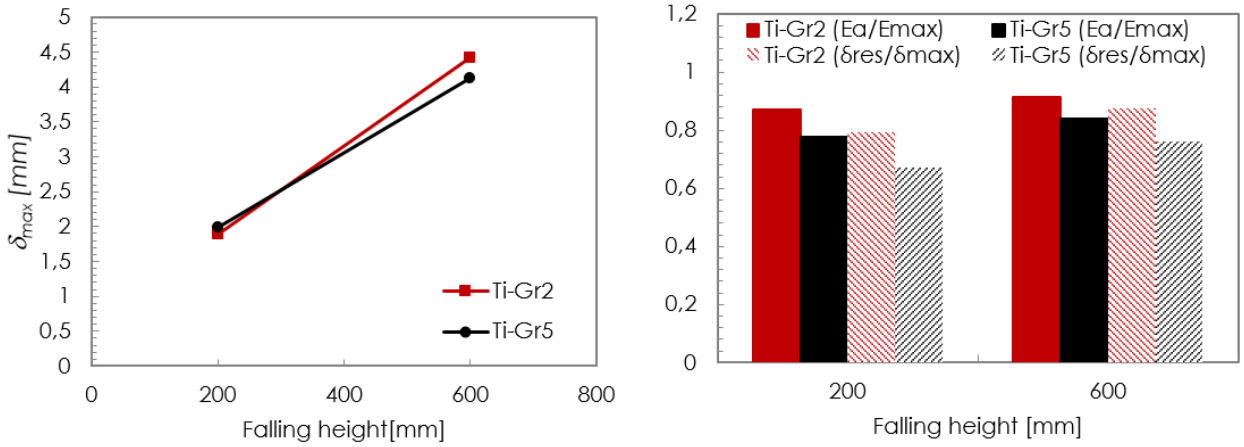

Figure 17. Comparison between SPIFed prostheses in Ti-Gr5 and Ti-Gr2 (1.5 mm thick).

Focusing the attention on the highest load conditions, results in Figure 16 and Figure 17 show that the implants in Ti-Gr5 (manufactured by both SPF and SPIF) exhibited the lowest capability to absorb energy and, consequently, the lowest deformation. This result is coherent with the results presented in Figure 11, which show that the Ti-Gr5 1.0 mm thick possesses a hardness level higher than the Ti-Gr23 1.0 mm thick; in a similar way, the Ti-Gr5 1.5 mm has a hardness level higher than the Ti-Gr2 1.5 mm thick.

It is also important to note that the preliminary hardness measurements can only be used to give an interpretation of the results and not to give a comprehensive evaluation of the

implant mechanical response. In fact, even though the hardness measurements revealed a marked difference between the Ti-Gr5 1.5 mm thick and the Ti-Gr2 1.5 mm thick, quite similar results were obtained for the Ti-Gr5 1.0 mm thick and the Ti-Gr23 1.0 mm thick. Moreover, data reported in Figure 16 and Figure 17 reveal, for both falling heights, a difference in terms of absorbed energy ratio and residual deflection ratio close to 9.5% and 14%, respectively.

3.3.2. Effect of the initial blank thickness

The graphs in Figure 18 show a direct comparison of the results in terms of the ratios E_a/E_{max} and $\delta_{res}/\delta_{max,}$ concerning the SPFed prostheses in Ti-Gr5 with a thickness of 1.0 mm and 1.5 mm subjected to the two load conditions.

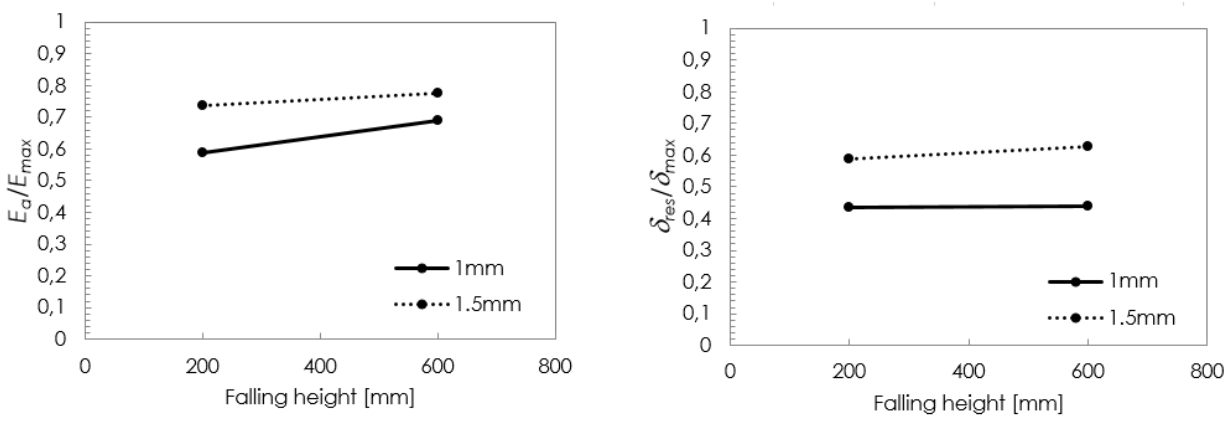

Figure 18. Comparison between prostheses in Ti-Gr5 with thickness 1.0 mm and 1.5 mm produced by SPF.

Figure 19 shows the same comparison but for the SPIFed prostheses in Ti-Gr5.

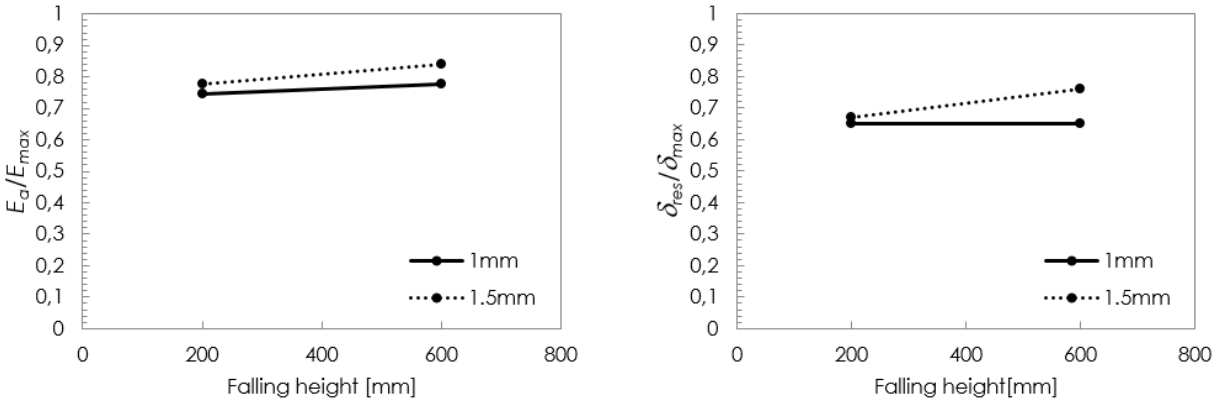

Figure 19. Comparison between prostheses in Ti-Gr5 with thickness 1.0 mm and 1.5 mm produced by SPIF.

Results in Figure 18 and in Figure 19 reveal that for the prostheses made by alloy TiGr5, as

observed during the impact tests performed on flat samples, the thicker the blank the lower the deflection and the higher the absorbed energy ratio. Such results reveal the possibility of assessing the effect of the initial blank thickness on drop test results simply using flat samples. However, it should be also highlighted that the exact values of the considered test parameters (the absorbed energy ratio and the deflection) strongly depend on the sample and, consequently, on the manufacturing process.

3.3.3. Effect of the manufacturing process

In Figure 20 results from tests conducted on both SPFed and SPIFed prostheses in Ti-Gr5 1.5 mm thick have been compared. Figure 20a shows the trend of the maximum force and of the maximum deflection after the impact (and the consequent rebound) for both load conditions.

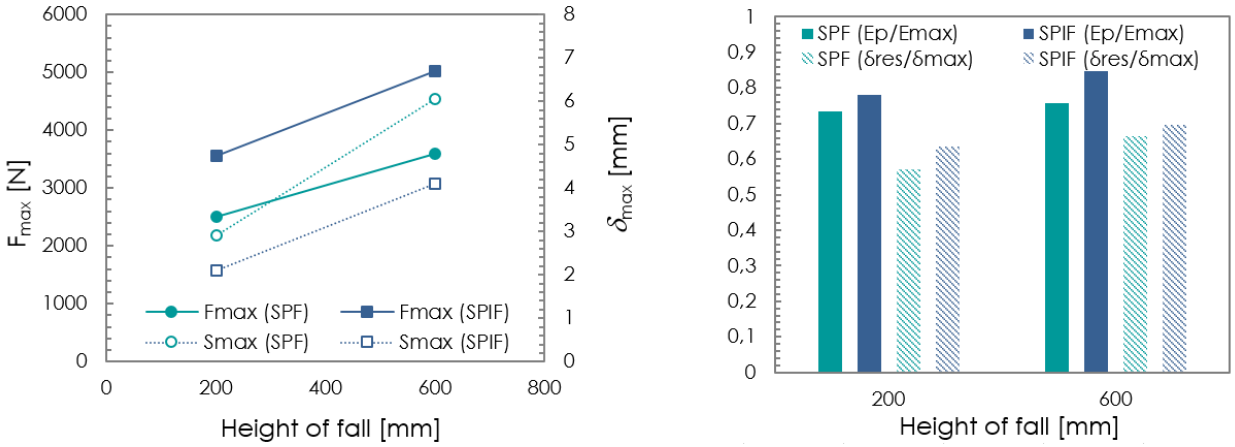

Figure 20. Comparison between prostheses in Ti-Gr5 (1.5 mm thick) produced by SPF and SPIF.

It can be noted that, in both testing cases, the implant produced by SPIF reached a maximum force about 40% larger than the one of the SPFed prosthesis (see continuous lines connecting full dots); in addition, SPIFed implants showed a maximum deflection δ_{max} smaller than the SPFed prosthesis one (when setting the falling height to 200mm, δ_{max} for the SPIFed prosthesis was about 40% lower than the SPFed one, whereas when setting the falling height to 600mm, δ_{max} for the SPIFed prosthesis was 48% lower than the SPFed one). These results reveal that the implant created by SPIF can be considered more rigid than the one produced by SPF, but it is worthy of notice that, as shown in Figure 20b, the residual deflection ratio and the absorbed energy ratio exhibited by the SPIFed prosthesis are, for both load conditions, higher than the ones reached by the SPFed prosthesis. In particular, for the falling height of 200mm, the deflection ratio and the energy ratio of the SPIFed prosthesis is about 10% and 6%, respectively, higher than the SPFed one. For the

falling height of 600mm, instead, these values are about 4% and 10%, respectively, higher than the SPFed one.

Such results could be related to the material alteration determined by the manufacturing processes. To evaluate this effect, the thickness distributions along the longitudinal section of the samples manufactured both by SPF and by SPIF have been measured and results have been plotted in Figure 20.

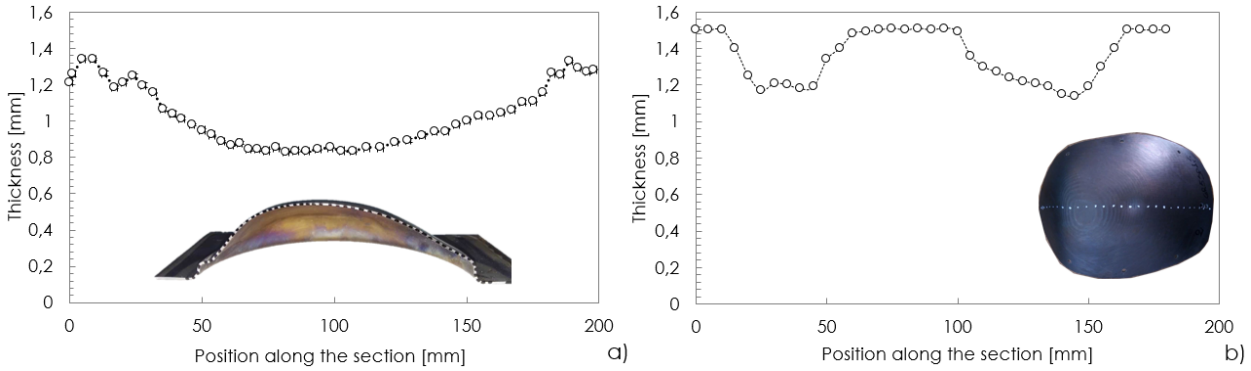

Figure 21. Thickness distribution along the longitudinal section of the sample manufactured by (a) SPF and (b) SPIF (initial sheet thickness 1.5mm).

It can be noted that the investigated processes have generated different thickness distributions and, as a consequence, a different mean value of the thickness. In particular, the SPIFed prosthesis, which is characterised by a mean thickness greater than the SPFed one, presents, in accordance with the results on flat samples, a lower maximum deflection and an higher maximum force.

On the contrary, the central region (where the impact load was applied) of the SPFed prostheses appears thinned (from 1.5 to 1.0 mm). Thus, in accordance with drop test data of flat samples, the thickness reduction, due to the manufacturing process, determined higher mechanical strength and, as a consequence, a lower level of the energy absorbed by the SPFed prosthesis (i.e. its capability to deform).

Finally, it can be concluded that, irrespective of the production process, the amount of energy absorbed by the implant was larger than 70% (at H=600mm: 76% for the SPF prosthesis, 85% for the SPIF prosthesis) while, at the same time, no fracture occurred in any implant after the impact.

4. Conclusions

The medical device market requests of new and more performing devices for the treatment of different pathologies are increasing every day. Consequently, the necessity of

investigating the mechanical reliability of implantable devices in the preclinical phase is becoming a more and more important activity, as to avoid that new devices are put into market without having demonstrated their safety. This lead to a continuous development and validation of new preclinical protocols that are often missing, especially for new devices.

In this manuscript, an additional brick of knowledge was introduced in the above mentioned direction: an innovative procedure was carefully designed for investigating the mechanical behaviour of titanium custom-made prostheses, manufactured by two innovative but well assessed technologies (Super Plastic Forming and Single Point Incremental Forming).

More deeply, the functional compatibility and the mechanical strength of the cranial implants were assessed by means of impact puncture tests. A specific set-up, using a purposely made PMMA anchoring support of geometry identical to the upper portion of the defected skull, was designed, fabricated and used since actually no standard exists in the literature.

The test assured an optimal repeatability and allowed to effectively determine the mechanical response of the implant, since no prosthesis failed in the anchoring region where self-cutting titanium cortical screws were used for fixing purposes. The test might be thus used for investigating how implants made of different Titanium alloys (Ti-Gr2, Ti-Gr5 and Ti-Gr23) behave when subjected to an impact load, even if they are characterized by different thickness values and manufactured using different processes.

Results from drop tests revealed to be in good agreement with the original mechanical behaviour of the investigated alloys (preliminary hardness tests), highlighting therefore that the adopted manufacturing process does not alter significantly the material characteristics. In the present experimental campaign, the tests allowed to demonstrate that, irrespective of the adopted manufacturing process, the amount of energy absorbed by the implants was always larger/greater than 70% (up to 85% for the prosthesis produced by Single Point Incremental Forming).

The proposed procedure for testing cranial prostheses can be extended to any geometry or material of the implant and can be successfully used to assess the effect of the manufacturing process.

Acknowledgements

The activities in this work were funded by the Italian Ministry of Education, Universities and Research Government through the PRIN Project 2012 “Biomedical Titanium alloy prostheses manufacturing by means of Superplastic and Incremental Forming processes” (project acronym: BIOFORMING).

References

[1] L.A. Pruitt, A.M. Chakravartula, Mechanics of Biomaterials: Fundamental Principles for Implant Design, Cambridge University Press, Cambridge, 2011. doi:DOI: 10.1017/CBO9780511977923.

[2] R.M. Wazen, J.A. Currey, H. Guo, J.B. Brunski, J.A. Helms, A. Nanci, Micromotion-induced strain fields influence early stages of repair at bone-implant interfaces, Acta Biomater. 9 (2013) 6663–6674. doi:10.1016/j.actbio.2013.01.014.

[3] J. Castelan, L. Schaeffer, A. Daleffe, D. Fritzen, V. Salvaro, F.P. Da Silva, Manufacture of custom-made cranial implants from DICOM?? images using 3D printing, CAD/CAM technology and incremental sheet forming, Rev. Bras. Eng. Biomed. 30 (2014) 265–273. doi:10.1590/rbeb.2014.024.

[4] H.R. Cho, T.S. Roh, K.W. Shim, Y.O. Kim, D.H. Lew, I.S. Yun, Skull reconstruction with custom made three-dimensional titanium implant, Arch. Craniofacial Surg. 16 (2015) 11–16. doi:10.7181/acfs.2015.16.1.11.

[5] H. Eufinger, M. Wehmöller, a Harders, L. Heuser, Prefabricated prostheses for the reconstruction of skull defects., Int. J. Oral Maxillofac. Surg. 24 (1995) 104–110. doi:10.1016/S0901-5027(05)80870-7.

[6] G. Staffa, A. Barbanera, A. Faiola, M. Fricia, P. Limoni, R. Mottaran, B. Zanotti, R. Stefini, Custom made bioceramic implants in complex and large cranial reconstruction: A two-year follow-up, J. Cranio-Maxillofacial Surg. 40 (2012) e65-70. doi:10.1016/j.jcms.2011.04.014.

[7] S.-C. Lee, C.-T. Wu, S.-T. Lee, P.-J. Chen, Cranioplasty using polymethyl methacrylate prostheses, J. Clin. Neurosci. 16 (2009) 56–63. doi:10.1016/j.jocn.2008.04.001.

[8] H.J. Rack, J.I. Qazi, Titanium alloys for biomedical applications, Mater. Sci. Eng. C. 26 (2006) 1269–1277. doi:10.1016/j.msec.2005.08.032.

[9] M. Niinomi, Mechanical biocompatibilities of titanium alloys for biomedical applications, J. Mech. Behav. Biomed. Mater. 1 (2008) 30–42. doi:10.1016/j.jmbbm.2007.07.001.

[10] M. Abdel-Hady Gepreel, M. Niinomi, Biocompatibility of Ti-alloys for long-term implantation, J. Mech. Behav. Biomed. Mater. 20 (2013) 407–415. doi:10.1016/j.jmbbm.2012.11.014.

[11] D.R. Calderoni, R. Gilioli, A.L.J. Munhoz, R. Maciel Filho, C.A.D.C. Zavaglia, C.S. Lambert, E.S.N. Lopes, I.F.C. Toro, P. Kharmandayan, Paired evaluation of calvarial reconstruction with prototyped titanium implants with and without ceramic coating.,

Acta Cir. Bras. 29 (2014) 579–587. doi:10.1590/S0102-8650201400150005.

[12] F.P.W. Melchels, J. Feijen, D.W. Grijpma, A review on stereolithography and its applications in biomedical engineering., Biomaterials. 31 (2010) 6121–30. doi:10.1016/j.biomaterials.2010.04.050.

[13] W.-M. Xi, A.-M. Wang, Q. Wu, C.-H. Liu, J.-F. Zhu, F.-F. Xia, An integrated CAD/CAM/robotic milling method for custom cementless femoral prostheses, Med. Eng. Phys. 37 (2015) 911–915. doi:10.1016/j.medengphy.2015.06.005.

[14] P. Kasprzak, G. Tomaszewski, G. Wróbel-Wiśniewska, M. Zawirski, Polypropylene-polyester cranial prostheses prepared with CAD/CAM technology. Report of first 15 cases., Clin. Neurol. Neurosurg. 113 (2011) 311–315. doi:10.1016/j.clineuro.2010.12.010.

[15] A. Piccininni, F. Gagliardi, P. Guglielmi, L. De Napoli, G. Ambrogio, D. Sorgente, Biomedical Titanium alloy prostheses manufacturing by means of Superplastic and Incremental Forming processes, 15007 (2016). doi:10.1051/matecconf/201.

[16] M.M. Landy, P.S. Walker, Wear of ultra-high-molecular-weight polyethylene components of 90 retrieved knee prostheses, J. Arthroplasty. 3 (1988) S73–S85. doi:10.1016/S0883-5403(88)80013-5.

[17] A. Toni, F. Giardina, G. Guerra, A. Sudanese, M. Montalti, S. Stea, B. Bordini, 3rd generation alumina-on-alumina in modular hip prosthesis: 13 to 18 years follow-up results, Hip Int. 27 (2017) 8–13. doi:10.5301/hipint.5000429.

[18] M. Junnila, I. Laaksonen, A. Eskelinen, P. Pulkkinen, L. Ivar Havelin, O. Furnes, A. Marie Fenstad, A.B. Pedersen, S. Overgaard, J. Kärrholm, G. Garellick, H. Malchau, K.T. Mäkelä, Implant survival of the most common cemented total hip devices from the Nordic Arthroplasty Register Association database, Acta Orthop. 87 (2016) 546–553. doi:10.1080/17453674.2016.1222804.

[19] A. Merini, A. Viste, R. Desmarchelier, M.H. Fessy, Cementless Corailtm femoral stems with laser neck etching: Long-term survival, rupture rate and risk factors in 295 stems, Orthop. Traumatol. Surg. Res. 102 (2016) 71–76. doi:10.1016/j.otsr.2015.10.009.

[20] A.R. Pelton, V. Schroeder, M.R. Mitchell, X.Y. Gong, M. Barney, S.W. Robertson, Fatigue and durability of Nitinol stents, J. Mech. Behav. Biomed. Mater. 1 (2008) 153–164. doi:10.1016/j.jmbbm.2007.08.001.

[21] M. Hasegawa, T. Azuma, Mechanical properties of synthetic arterial grafts, J. Biomech. 12 (1979) 509–517. doi:10.1016/0021-9290(79)90039-3.

[22] S. Kapila, R. Sachdeva, Mechanical properties and clinical applications of orthodontic wires., Am. J. Orthod. Dentofac. Orthop. 96 (1989) 100–9. doi:http://dx.doi.org/10.1016/0889-5406(89)90251-5.

[23] B. Zanotti, N. Zingaretti, A. Verlicchi, M. Robiony, A. Alfieri, P.C. Parodi, Cranioplasty, J. Craniofac. Surg. 27 (2016) 2061–2072. doi:10.1097/SCS.0000000000003025.

[24] ISO 7206-4:2010, Implants for surgery -- Partial and total hip joint prostheses -- Part 4: Determination of endurance properties and performance of stemmed femoral

components., (n.d.).

[25] ISO 12189:2008, Implants for surgery -- Mechanical testing of implantable spinal devices -- Fatigue test method for spinal implant assemblies using an anterior support, (n.d.).

[26] ASTM F732 - 00(2011), Standard Test Method for Wear Testing of Polymeric Materials Used in Total Joint Prostheses, (n.d.).

[27] ASTM F1801 - 97(2014), Standard Practice for Corrosion Fatigue Testing of Metallic Implant Materials, (n.d.).

[28] A. Tsouknidas, S. Maropoulos, S. Savvakis, N. Michailidis, FEM assisted evaluation of PMMA and Ti6Al4V as materials for cranioplasty resulting mechanical behaviour and the neurocranial protection, Biomed. Mater. Eng. 21 (2011) 139–147. doi:10.3233/BME-2011-0663.

[29] D. Garcia-Gonzalez, J. Jayamohan, S.N. Sotiropoulos, S.H. Yoon, J. Cook, C.R. Siviour, A. Arias, A. Jérusalem, On the mechanical behaviour of PEEK and HA cranial implants under impact loading, J. Mech. Behav. Biomed. Mater. 69 (2017) 342–354. doi:10.1016/j.jmbbm.2017.01.012.

[30] C. Ciancio, M.V. Caruso, G. Fragomeni, G. Ambrogio, Integrated thermomechanical model for forming glass containers, MATEC Web Conf. 80 (2016) 16010-1-16010–6. doi:10.1051/matecconf/201.

[31] UNI EN ISO 6507, Metallic materials - Vickers hardness test - Part 1: Test method, (n.d.).

[32] H.-S. Lee, J.-H. Yoon, C.H. Park, Y.G. Ko, D.H. Shin, C.S. Lee, A study on diffusion bonding of superplastic Ti–6Al–4V ELI grade, J. Mater. Process. Technol. 187–188 (2007) 526–529. doi:10.1016/j.jmatprotec.2006.11.215.

[33] D. Sorgente, G. Palumbo, A. Piccininni, P. Guglielmi, L. Tricarico, Modelling the superplastic behaviour of the Ti6Al4V-ELI by means of a numerical/experimental approach, Int. J. Adv. Manuf. Technol. 90 (2017) 1–10. doi:10.1007/s00170-016-9235-7.

[34] ASTM Standard D. 7136; 2005, Standard test method for measuring the damage resistance of a fiberreinforced polymer matrix composite to a drop-weight impact event, (n.d.).